Dynamics of quantum coherence and nonlocality of a two-spin system in the chemical compass

Y. Aiache ,[1,*] K. El Anouz,[1] N. Metwally ,[2,3] and A. El Allati [1,4]

[1] *Laboratory of R&D in Engineering Sciences, Faculty of Sciences and Techniques Al-Hoceima, Abdelmalek Essaadi University, BP 34. Ajdir 32003, Tetouan, Morocco*

[2] *Mathematics Department College of Science, University of Bahrain, Sakhir, PO Box 320038, Bahrain*

[3] *Department of Mathematics, Aswan University, Aswan, Sahari 81528, Egypt*

[4] *Max Planck Institute for the Physics of Complex Systems, Nöthnitzer Str. 38, D-01187 Dresden, Germany*

(Received 9 December 2023; accepted 9 February 2024; published 1 March 2024)

In this paper a system consisting of two electron spins has been prepared initially in a singlet state using the chemical compass model is considered. It is assumed that each electron spin interacts symmetrically and/or asymmetrically with its respective private nuclear environment in the presence of an external magnetic field. We discussed the effect of the interaction parameters and the external magnetic field on some quantifiers of quantum correlations as entanglement, coherence, Bell inequality, as well as the steerability inequality. It is shown that within a certain range of external magnetic fields, the quantum coherence and entanglement behave similarly. The Bell and the steerable inequalities predicted a similar behavior for symmetric and asymmetric interactions. Moreover, as one increases the external magnetic field, the lower bounds of both inequalities have improved. The usefulness of using the spin state as quantum channel to teleport a two-qubit system has examined where the Bell inequality could be above its classical bounds by controlling the interaction parameters. It is shown that by tuning the coupling parameters the fidelity of the teleported state exceeds the classical bounds, as well as the long-lived stationary fidelity could be achieved during the interaction time.

DOI: 10.1103/PhysRevE.109.034101

I. INTRODUCTION

Over the years, a significant amount of experimental evidence has consistently demonstrated the influence of magnetic fields on chemical reactions [1–3], constructing the foundations of radical pair mechanism development. This mechanism, which originated in the 1970s, sheds light on how external magnetic fields can affect chemical reactions induced by light. As a result, spin chemists have invested major resources in studying these reactions in molecular systems [4,5], with particular emphasis on their sensitivity to both light and magnetic fields. Furthermore, some aspects of the radical pair mechanism share commonalities with components found in quantum computing methods and quantum communication protocols. For example, after photoexcitation and charge transfer, the initial state of the radical pair assumes a spin singlet configuration, which is a maximally entangled Bell state. This configuration serves as a valuable resource for various quantum information tasks, including dense coding capacity [6,7], quantum state teleportation [8–11], and quantum key distribution [12,13]. Through the presence of the external magnetic field and that of the nuclear spins, the spin state of the radical pair changes. The observed similarities raise the question of whether magnetic field sensing based on the radical pair mechanism can be understood as a fundamental form of quantum information processing.

Correlations resulting from local measurements on entangled quantum systems may exhibit nonlocal correlations [14]. Significantly, the local hidden variable model imposes restrictions on the measurement statistics for a sufficiently large collection of quantum systems [8]. Nonlocality, as an important concept, has its origins in the EPR paradox, which is at the heart of nonlocality [15]. This paradox challenges the idea that quantum mechanics can allow what is commonly known as spooky action at a distance. Subsequently, Schrödinger explained this phenomenon by suggesting that local measurements could influence distant quantum subsystems without direct access, a concept referred to as quantum steering, often called EPR steering [16]. In general, quantum steering serves as a quantification of the quantum correlations that exemplified the EPR paradox. Particularly, it is recognized in modern quantum information theory as a measure of the quantum correlations between quantum entanglement and Bell nonlocality. Moreover, steerable states are considered to be a subset of entangled states [17]. Recently, quantum steering has gained considerable attention in both theoretical and experimental research [18–23].

The aim of our research is to examine the radical pair mechanism and the chemical compass model, using several techniques and methods from quantum information. An extensively studied example of spin chemistry is a solution containing pyrene (Py) and dimethylaniline (DMA), where DMA serves as a donor and Py as an acceptor [24]. Magnetic field-dependent effects have been extensively studied for this pair of molecules, including studies of isotope effects [4,25]. This study focuses on a quantum system consisting of two unpaired electrons in a spin-correlated electronic singlet state within a radical pair, with each electron interacting with its respective private environment. First, we investigate quantum

[*] youssefaiache0@gmail.com

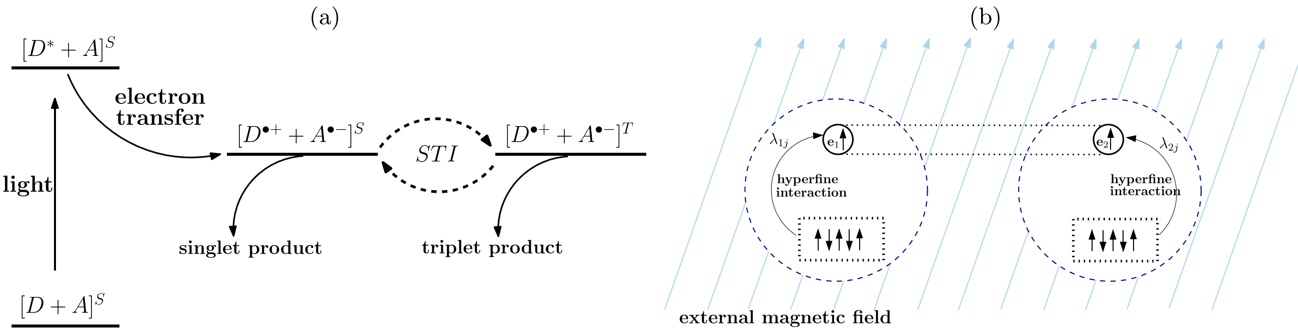

FIG. 1. (a) Schematic of the radical-pair mechanism. After light-induced electron transfer, donor (D), and acceptor (A) molecules form a correlated spin radical pair. The magnetic field causes the spin character of the radical spins to interconversion between singlet and triplet states. (b) The diagram shows two electron spins, e_1 and e_2. Both electron spins interact with their respective nuclear environments through hyperfine interactions. In addition, the pair of electrons is affected by the Zeeman effect caused by an external magnetic field.

coherence against entanglement by means of concurrence. Our results show that by manipulating the hyperfine couplings between the electrons and their corresponding environments, as well as an external magnetic field, coherence and concurrence exhibit similar behavior. In particular, the external magnetic field provides an opportunity to enhance and control the lifetime of entanglement, showing that it promotes the growth of entanglement and quantum coherence without causing their destruction. Next, we will explore the nonlocality in this model, including quantum steering and Bell nonlocality, and examine the delicate dependence between these different measures of nonlocality. Finally, we will study quantum teleportation in the model, taking into account the violation of Bell nonlocality, to establish the relationship between quantum teleportation and the violation of Bell nonlocality.

The paper is organized as follows. The considered two-electron-spin physical model is presented in Sec. II. Definitions and mathematical formulas for concurrence, coherence, Bell nonlocality, and quantum steering, along with their dynamical behavior and discussion, are presented in Secs. III and IV, respectively. Quantum teleportation is discussed in Sec. V. The paper is finished with a conclusion of the current investigation in Sec. VI.

II. DESCRIPTION OF THE MODEL

Let us consider a spin-correlated radical pairs consisting of a donor (D) and an acceptor (A), as illustrated in Fig. 1. Initially, the two unpaired electrons have their spins in a singlet state. The behavior of the radical pair spins over time is determined by the intensity of the external magnetic field and the interaction with the nuclear spins in the molecule, which are assumed to be isotropic. In this context, we can describe the spin Hamiltonian for a radical pair, including both hyperfine and Zeeman interactions. The total Hamiltonian of the system can be presented in a general form as below [26]

$$H = \mu_B(g_1\mathbf{B}.\,\mathbf{S}_1 + g_2\mathbf{B}.\,\mathbf{S}_2) + \sum_{j=1}^{N_1 N_2} \mu_B(g_1\mathbf{S}_1.\,\boldsymbol{\lambda}_{1,j}.\,\mathbf{I}_{1,j} + g_1\mathbf{S}_2.\,\boldsymbol{\lambda}_{2,j}.\,\mathbf{I}_{2,j}), \quad (1)$$

where the first term in the right-hand side of Eq. (1) is the Hamiltonian of Zeeman interaction. It refers to the interaction of electron spins with an external magnetic field $\mathbf{B}$. However, the second term represents the hyperfine Hamiltonian, which describes the interaction between the electrons and the nuclei of the molecule. However, μ_B indicates the Bohr magneton, $g_1 = g_2 = 2$ denotes the effective g factor of electrons e_1 and e_2, and $\mathbf{S}$ signifies the dimensionless electron spin operators, defined as $\boldsymbol{\sigma}/2$ with $\boldsymbol{\sigma}$ being the vector of Pauli matrices. Additionally, $\boldsymbol{\lambda}_{1,j}$ and $\mathbf{I}_{1,j}$ represent the hyperfine coupling tensor and nuclear spin of the jth nucleus. For simplicity, we assume that each electron is coupled to one proton.

The assumption that each electron spin interacts solely with its respective environmental nuclei allows us to separate the temporal evolution of the system into the separate evolution of the two radicals [see Fig. 1(b)]. The only factor linking these two radicals, and necessitating their simultaneous treatment, is their initial correlated state. The dynamics of the electron spin states are governed according to Eq. (1) as

$$\rho(t) = \mathrm{Tr}_{\mathrm{nuc}}\left[\mathcal{U}(t)\left(\rho(0) \otimes \frac{\mathbb{1}}{d_{\mathrm{nuc}}}\right)\mathcal{U}^\dagger(t)\right], \quad (2)$$

where the nuclear spin environment is traced from the initial evolved state of the whole system, where d_{nuc} is the Hilbert space dimension of the nuclear spins and $\mathcal{U}(t) = \mathrm{Exp}(-iHt/\hbar)$. However, when the spins of two electrons, labeled by S_{e_1} and S_{e_2}, combine, they result in a total spin, labeled by S_T, with a quantum number of either $S = 1$ or $S = 0$. In the latter case, it is referred to as a singlet state, with $m_s = 0$, while in the former case, it is referred to as a triplet state, with $m_s = 0, \pm 1$

$$|S\rangle = (|\uparrow\downarrow\rangle - |\downarrow\uparrow\rangle)/\sqrt{2},$$
$$|T_0\rangle = (|\uparrow\downarrow\rangle + |\downarrow\uparrow\rangle)/\sqrt{2},$$
$$|T_+\rangle = |\uparrow\uparrow\rangle, \quad |T_-\rangle = |\downarrow\downarrow\rangle. \quad (3)$$

We employ the standard assumption and consider a singlet state denoted by $\rho(0) = |S\rangle\langle S|$ as the initial state for the electron spins.

Figure 2 illustrates how the hyperfine interaction caused by the nuclei begins to mix the spin properties of the electron spins, alongside the transformation driven by the external magnetic field. Specifically, as shown in Fig. 2(a), when the external magnetic field is zero, the singlet fidelity is initially maximized. As the interaction is switched on, it decreases, and

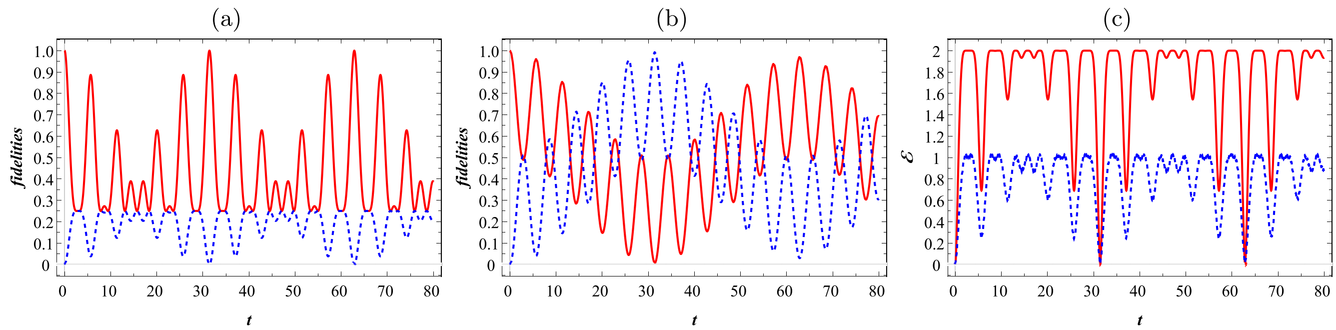

FIG. 2. An illustration of the singlet-triplet (T_0) fidelities and von Neumann entropy ($\mathcal{E}$) for fixed hyperfine coupling, i.e., $\lambda_{1,1} = 0.5$ and $\lambda_{2,1} = 0.6$. (a) singlet- (red line) and triplet-zero fidelity (blue dashed line) in the absence of the external magnetic field $\mathbf{B} = 0$. (b) same as Fig. 2(a) but in the presence of the external magnetic field $\mathbf{B} = 10$. Finally, (c) reflects von Neumann entropy, where $\mathbf{B} = 0$ and $\mathbf{B} = 10$ hold for the red line and blue dashed line, respectively.

in the meantime, the triplet fidelity increases until it reaches its maximum value, which is 0.25. At the same time, the singlet state reaches its minimum value, which is also 0.25. As time progresses, the triplet fidelity oscillates between 0 and the minimum value of the singlet fidelity. However, this is not the case in the presence of the external magnetic field, namely $\mathbf{B} = 10$. As shown in Fig. 2(b) the system is no longer in the singlet state, indicating an interconversion between the singlet and triplet states. More specifically, at $t = 0$, the system is in a singlet state, but due to the effect of the magnetic field, at $t = 31.35$, the system transitions into a triplet state.

The rise in von Neumann entropy, which results from the mixing induced by the decohering environment of nuclei and the associated loss (and recovery) of singlet coherence, is visually depicted in Fig. 2(c). Initially, the entropy is at zero, signifying that the system is well defined, i.e., in a pure state, as indicated in Fig. 2(a), that is singlet state. On the one hand, in the absence of an external magnetic field [as shown in the red behavior in Fig. 2(c)], the maximal entropy value is 2, which indicates that the quantum state is a completely mixed state. Furthermore, when we compare von Neumann entropy and singlet fidelity behaviors, it is remarkable that a decrease in singlet fidelity corresponds to an increase in von Neumann entropy, meaning that the degree of uncertainty increases, and vice versa. On the other hand, the presence of an external magnetic field reduces the mixture in the quantum system, as evidenced by the von Neumann entropy in Fig. 2(c). This can be explained as the interconversion of singlet-triplet states caused by the external magnetic field. However, from Figs. 2 and 3 it is evident that the increase in the numbers of hyperfine coupling is resulting in an increase in the oscillations in both singlet-triplet fidelities and von Neumann entropy.

III. QUANTUM CORRELATIONS: PRELIMINARIES

In this section, we will recall the main definitions and mathematical framework of the quantum correlation measures that will be used in this study. These quantifiers include coherence, concurrence, Bell nonlocality, and quantum steering.

A. Coherence versus entanglement

Quantum coherence, which arises from quantum superposition, plays a crucial role in quantum mechanics. It serves as a fundamental property for both entanglement and other forms of quantum correlations. In addition, it is a crucial resource in the fields of quantum computation and quantum information processing. A variety of methods are available to quantify quantum coherence, with the ℓ_1 norm of coherence being a widely used approach in quantum physics. This measure is expressed as [27]

$$\mathcal{C}_l = \sum_{i \neq j} |\rho_{ij}|. \tag{4}$$

To characterize the quantum entanglement in the reduced density matrix $\rho(t)$, we use the commonly employed measure known as concurrence $\mathcal{C}$ for a two-spin system. This measure was originally introduced by Wootters [28]. A value of $\mathcal{C} = 0$

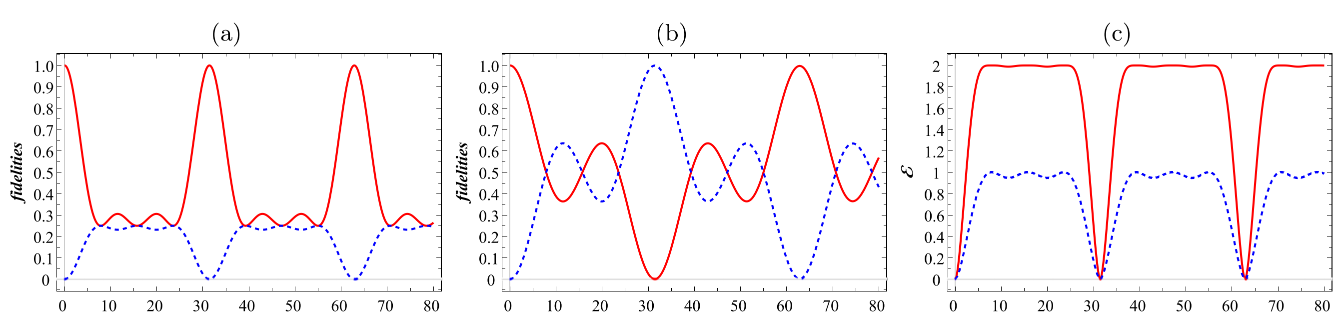

FIG. 3. The same as Fig. 2 but the hyperfine couplings are $\lambda_{1,1} = 0.1$ and $\lambda_{2,1} = 0.2$.

indicates that the state of the system is separable, while a value of $\mathcal{C} = 1$ indicates that the system is maximally entangled. An explicit definition of concurrence can be formulated as follows:

$$\mathcal{C} = \max\{0, \sqrt{\delta_1} - \sqrt{\delta_2} - \sqrt{\delta_3} - \sqrt{\delta_4}\}, \tag{5}$$

where $\delta_i (i = 1, 2, 3, 4)$ represent the eigenvalues of the matrix $\mathcal{R} = \rho(t)(\sigma_y \otimes \sigma_y)\rho^*(t)(\sigma_y \otimes \sigma_y)$ in decreasing order, while $\rho^*(t)$ is the complex conjugated of $\rho(t)$.

B. Bell nonlocality

To achieve a better understanding of quantum correlations, it is crucial to establish the Bell–Clauser-Horne-Shimony-Holt (Bell-CHSH) inequality in a simplistic form. In order to study nonlocality within the CHSH framework, we can use the Bell operator, as described in Ref. [29]. Consequently, the definition of the Bell-CHSH inequality is as follows [30]:

$$\mathcal{B}_{\text{CHSH}} = a \cdot \sigma \otimes (b + b') \cdot \sigma + a' \cdot \sigma \otimes (b - b') \cdot \sigma, \tag{6}$$

where a, a', b, b' are unit vectors, and $\sigma = (\sigma_x, \sigma_y, \sigma_z)$ is the vector of Pauli matrices. The CHSH inequality can be formulated for any bipartite mixed state using the following expression:

$$|\text{Tr}\{\rho(t)\mathcal{B}_{\text{CHSH}}\}| \leqslant 2. \tag{7}$$

The CHSH inequality is satisfied for any state that can be explained by a local hidden variable model. If the inequality is violated, it means the Bell nonlocality of the underlying state. The maximum violation of Bell's inequality can also be expressed as follows [31]:

$$\mathcal{B} = 2\sqrt{t_i + t_j}, \tag{8}$$

where t_i and t_j are the two biggest eigenvalues of the matrix $\mathcal{T}^\dagger\mathcal{T}$, where $\mathcal{T}$ is the correlation matrix with elements $t_{kl} = \text{Tr}[\rho(t)\sigma_k \otimes \sigma_l]$ with $\{k, l\} = \{1, 2, 3\}$.

C. Quantum steering

The basic concept of the steering phenomenon stems from the mysterious features of quantum mechanics explored by Einstein-Podolsky-Rosen and Schrödinger. Nevertheless, the steering phenomenon in two-qubit states can be quantified by steering inequalities, using the Cavalcanti-Jones-Wiseman-Reid (CJWR) inequality [32,33]. Taking into account three measurements, the CJWR inequality can be defined as:

$$F_{\text{CJWR}}(\rho(t), r) = \frac{1}{\sqrt{3}}\left|\sum_{i=1}^{3} \langle A_i \otimes B_i\rangle\right| \leqslant 1, \tag{9}$$

where $A_i = r_i^A.\boldsymbol{\sigma}$ and $B_i = r_i^B.\boldsymbol{\sigma}$ indicate the projections correspond to the measurements carried out on Alice and Bob, respectively. The set $r = r_i^A, r_i^B$ denotes the measurement directions. If we take into account the maximum values of $F_{\text{CJWR}}(\rho(t), r)$, denoted by $F(\rho(t))$, then Eq. (9) can be reformulated as follows [34]:

$$\mathcal{QS} = F(\rho(t)) = \sqrt{t_1^2(\rho(t)) + t_2^2(\rho(t)) + t_3^2(\rho(t))} \leqslant 1, \tag{10}$$

where $t_1(\rho(t))$, $t_2(\rho(t))$, $t_3(\rho(t))$ are the eigenvalues of the correlation matrix $\mathcal{T}$ (more details are given in Sec. III B).

IV. RESULTS AND DISCUSSION

A. Coherence versus entanglement

In this section, we will investigate the effect of the external magnetic field **B** and the influence of hyperfine coupling in the proposed system, namely two electrons where each electron is interacting with its own environment (we assume that each electron is coupled to one proton) on coherence and entanglement. It is obvious that in the absence of an external magnetic field [as shown in Fig. 4(a)] that the existence of coherence in the quantum system does not guarantee the presence of entanglement. More specifically, one can see that as the coherence takes different values in the ranges of [0,0.33], the spin system is separable, where the concurrence remains zero, but as the values of coherence cross the threshold, i.e., $\mathcal{C}_l \approx 0.33$ there is a corresponding increase in the values of entanglement, and eventually both coherence and entanglement reach their maximum values. This is because the system is initially prepared in a singlet state. However, as the external magnetic field is switched on [as shown in Figs. 4(b) and 4(c)] there is an enhancement in the entanglement, specifically, in the case where $\mathbf{B} = 0.05$ there is a sudden increase in the entanglement in a value of coherence, namely $\mathcal{C}_l \approx 0.29$ but they ($\mathcal{C}_l$ and $\mathcal{C}$) can not reach their maximum due to the effect of decoherence imposed by the nuclei environment. Moreover, in the case when the two-hyperfine coupling imposed by each proton on its respective electron is almost equal (symmetric), i.e., $\lambda_{1,1} = 0.2 \approx \lambda_{2,1}$ (as illustrated in the small plot in Fig. 4(b)], there is a marked increase of oscillation and their magnitude in the behavior of $\mathcal{C}_l$ and $\mathcal{C}$. However, Fig. 4(c) displays the same quantities and parameters as in Fig. 4(b), but for $\mathbf{B} = 0.1$ as before, we observe a sudden rise of entanglement in a situation where $\mathcal{C}_l \approx 0.18$. Moreover, when the values of $\lambda_{1,1}$ and $\lambda_{2,1}$ are approximately identical (symmetry interaction), i.e., $\lambda_{2,1} \approx \lambda_{1,1} = 0.2$ there is an enhancement of oscillation and their magnitude [see the small plot in Fig. 4(c)]. In a scenario where $\mathbf{B} = 10$ in Fig. 4(d), it is evident to say that the existence of an external magnetic field with large values results in an improvement of entanglement between two electron spins. Furthermore, in this case, the coherence implies the existence of entanglement. From Fig. 5 it is obvious that the presence of the external magnetic field improves quantum correlations in the two electron spins. Moreover, the existence of coherence does not necessarily ensure that entanglement can be obtained.

B. Quantum steering and Bell nonlocality

In this section, we investigate the sensitivity of quantum steering and Bell nonlocality in Figs. 6 and 7, respectively. These measures allow us to quantify quantum correlations between the two electron spins in the radical pair. We also discuss the effect of the absence and presence of the external magnetic field and the hyperfine couplings on the behavior of these quantities during the interaction. However, Fig. 6(a), where we consider a symmetry interaction, i.e., $\lambda_{1,1} \approx \lambda_{2,1} = 0.2$ and Fig. 6(b), where an asymmetry interaction is taken into account, i.e., $\lambda_{1,1} = 0.2$, $\lambda_{2,1} = 0.1$ display the effect of the external magnetic field on quantum steering. Moreover, it is obvious that the behavior of the latter is initially maximized

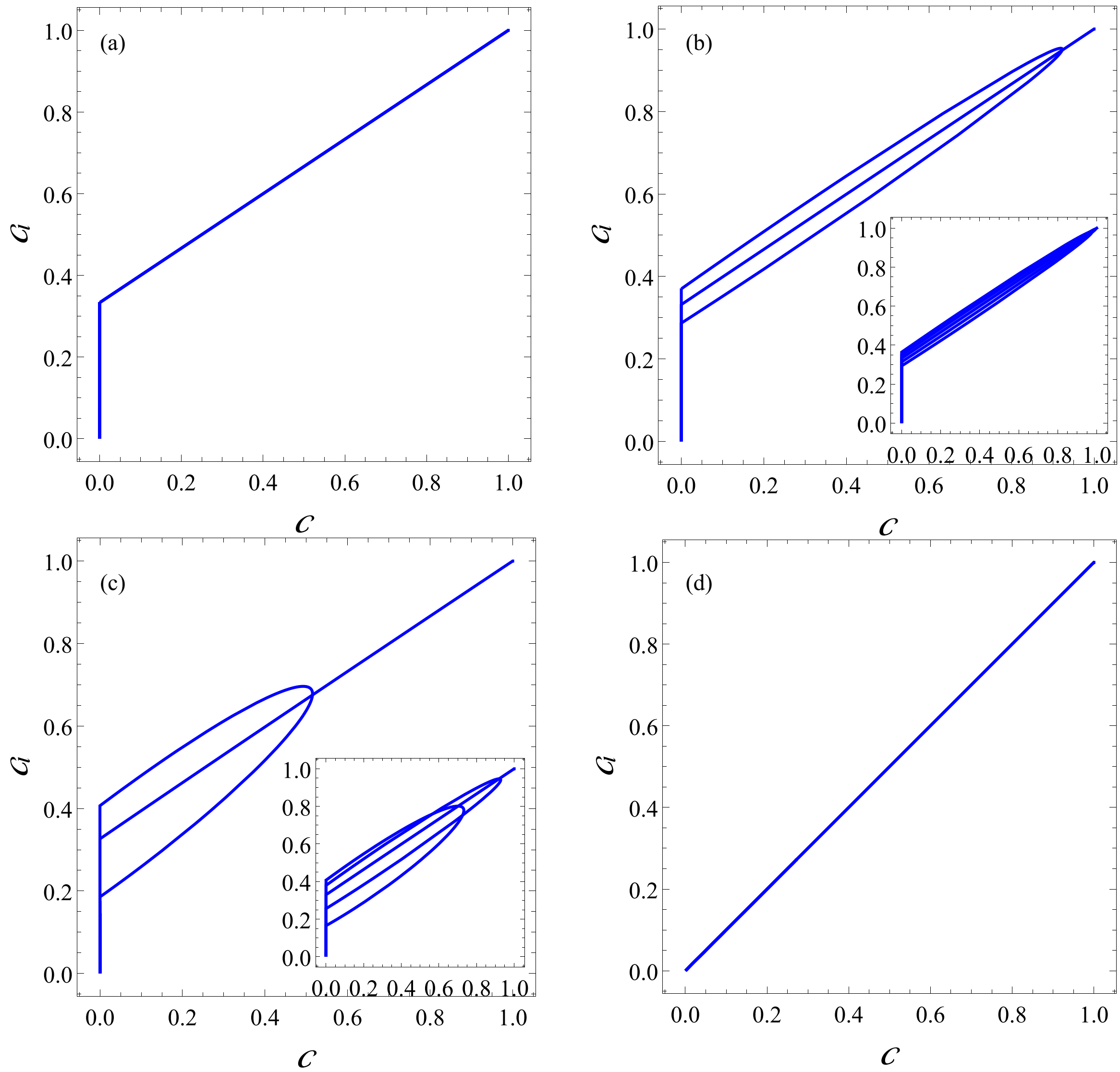

FIG. 4. Parametric plot of coherence ($\mathcal{C}_l$) versus concurrence ($\mathcal{C}$) for fixed $\lambda_{1,1} = 0.2$, $\lambda_{2,1} = 0.1$, (a) in the absence of external magnetic field $\mathbf{B} = 0$, (b) for $\mathbf{B} = 0.05$, (c) for $\mathbf{B} = 0.1$ and (d) for $\mathbf{B} = 10$. The small subfigures in (b) and (c) for symmetry interaction are $\lambda_{1,1} = 0.2 \approx \lambda_{2,1}$.

due to the fact that the system is initially prepared in a singlet state. Furthermore, as the interaction is switched on, specifically in the interval $t \in]0, 7.5]$, quantum steering decreases as time interaction increases; moreover, as the external magnetic field takes the values 0, 0.05, and 0.1 quantum steering decreases rapidly, eventually falling below its classical limits, which is one. However, this is not the case when $\mathbf{B} = 10$, quantum steering decreases in a manner quite slower and eventually becomes steady at a value identical to the classical limits. However, in the interval $t \in]7.5, 23.5]$ there is a sudden rise of quantum steering, specifically, on one hand when the hyperfine couplings take values, namely $\lambda_{1,1} = 0.2$ and $\lambda_{2,1} = 0.1$ as depicted in Fig. 6(b), there is a small increase in quantum steering when $\mathbf{B} = 10$ and for other values, quantum steering remains below its classical limit.

On the other hand, when $\lambda_{1,1}$ and $\lambda_{2,1}$ are nearly identical, the behavior shows a periodical increasing as time interaction increases, and this can be interpreted as follows: the simplified model, with only two nuclear spins, illustrates the reemergence of the initial state after a certain time, determined by the two identical hyperfine couplings and the external magnetic field, as shown in Figs. 2 and 3. A two-nucleus serves as a very limited environment, resulting in a decay rate smaller compared to the one found in the paper [35].

In other words, the environment has a limited information capacity. Consequently, the dynamics of the system quickly returns it to its initial state, facilitated by the small environment, which effectively feeds back the information lost from the system to the environment as a result of decoherence. Furthermore, Figs. 6(c) and 6(d) illustrate the effect of hyperfine couplings on quantum steering in the absence and presence of an external magnetic field, respectively. However, in the absence of $\mathbf{B}$ quantum steering is at its maximum and decreases rapidly as $\lambda_{2,1}$ takes a large value, i.e., 0.5, whereas for the small values, quantum steering slowly decreases. Moreover, the sudden death or birth phenomena of quantum steering are caused by its sensitivity to the decoherence phenomenon. Furthermore, from Fig. 6(d), the maximum and minimum bounds

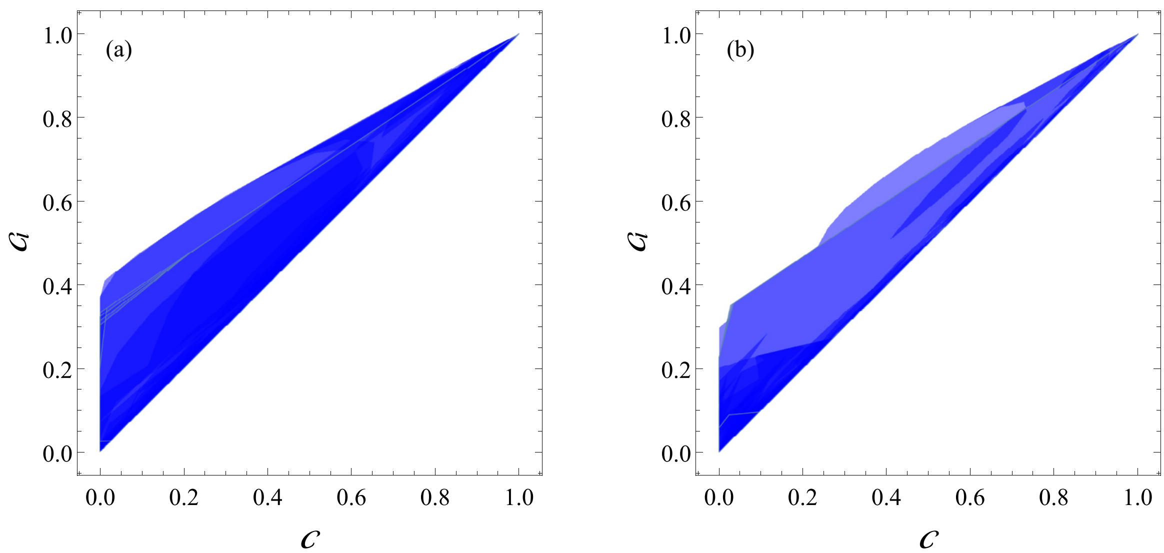

FIG. 5. Parametric plot of coherence ($\mathcal{C}_l$) versus concurrence ($\mathcal{C}$), where $\mathbf{B} \in [0, 10]$. Moreover, (a) for $\lambda_{1,1} = 0.2 \approx \lambda_{2,1}$ and (b) for $\lambda_{1,1} = 0.2$, $\lambda_{2,1} = 0.1$.

of quantum steering are determined by appropriate values of the external magnetic field and hyperfine coupling.

We have illustrated in Fig. 7 the time variation of the Bell nonlocality, $\mathcal{B}$, in the absence and presence of an external magnetic field for the symmetry and asymmetry interaction between the electrons and their corresponding environment. However, the general behavior of Bell nonlocality is similar to that shown for the inequality of the quantum steering. The two quantities initially decrease from the maximum value at $t = 0$, where the singlet state is maximally steerable with perfect

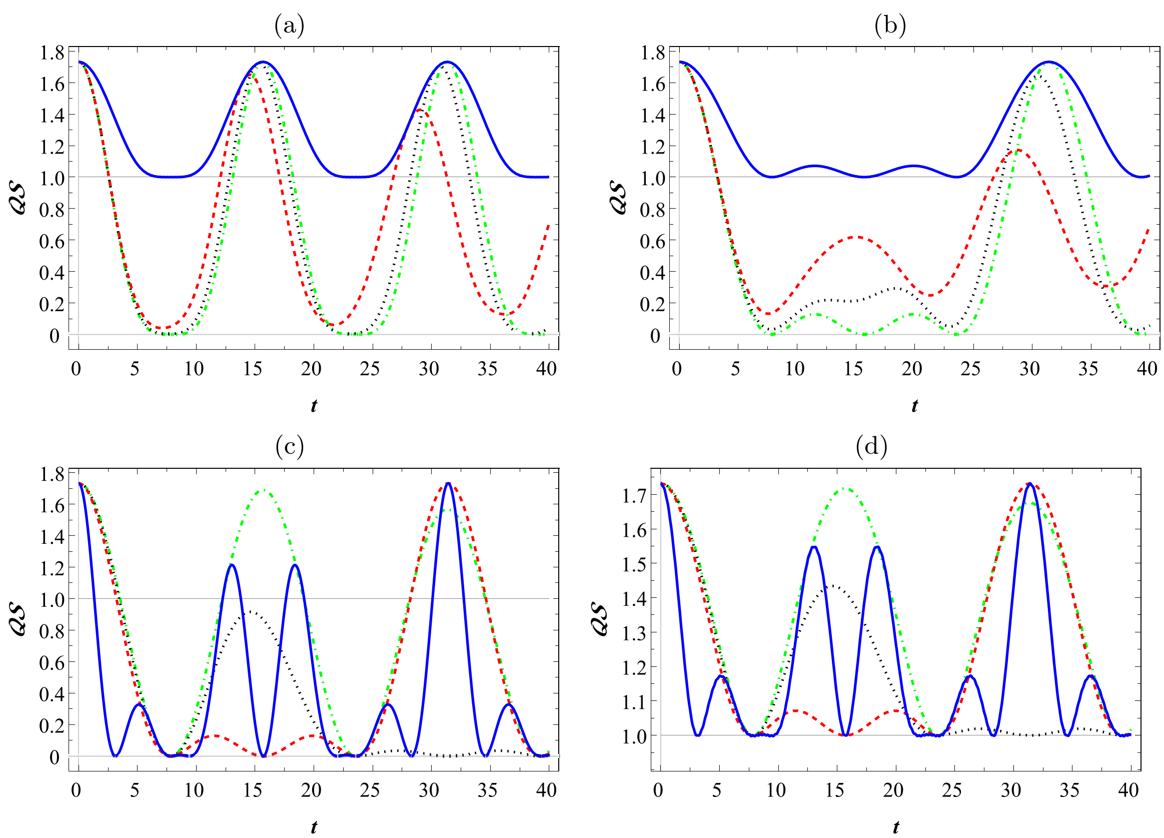

FIG. 6. Quantum steering (a) for a symmetric interaction, i.e., $\lambda_{1,1} = 0.2 \approx \lambda_{2,1}$, where $\mathbf{B} = 0,\ 0.05,\ 0.1$, and $\mathbf{B} = 10$ stand for green dotted-dashed, black dotted, red dashed, blue solid lines, respectively, (b) same as Fig. 6(a) but $\lambda_{1,1} = 0.2$, $\lambda_{2,1} = 0.1$, (c) for $\lambda_{2,1} = 0.2$ and $\mathbf{B} = 0$, where $\lambda_{1,1} = 0.01,\ 0.05,\ 0.1$, and $\lambda_{1,1} = 0.5$ stand for green dotted-dashed, black dotted, red dashed, blue solid lines, respectively, (d) same as Fig. 6(c) but $\mathbf{B} = 10$.

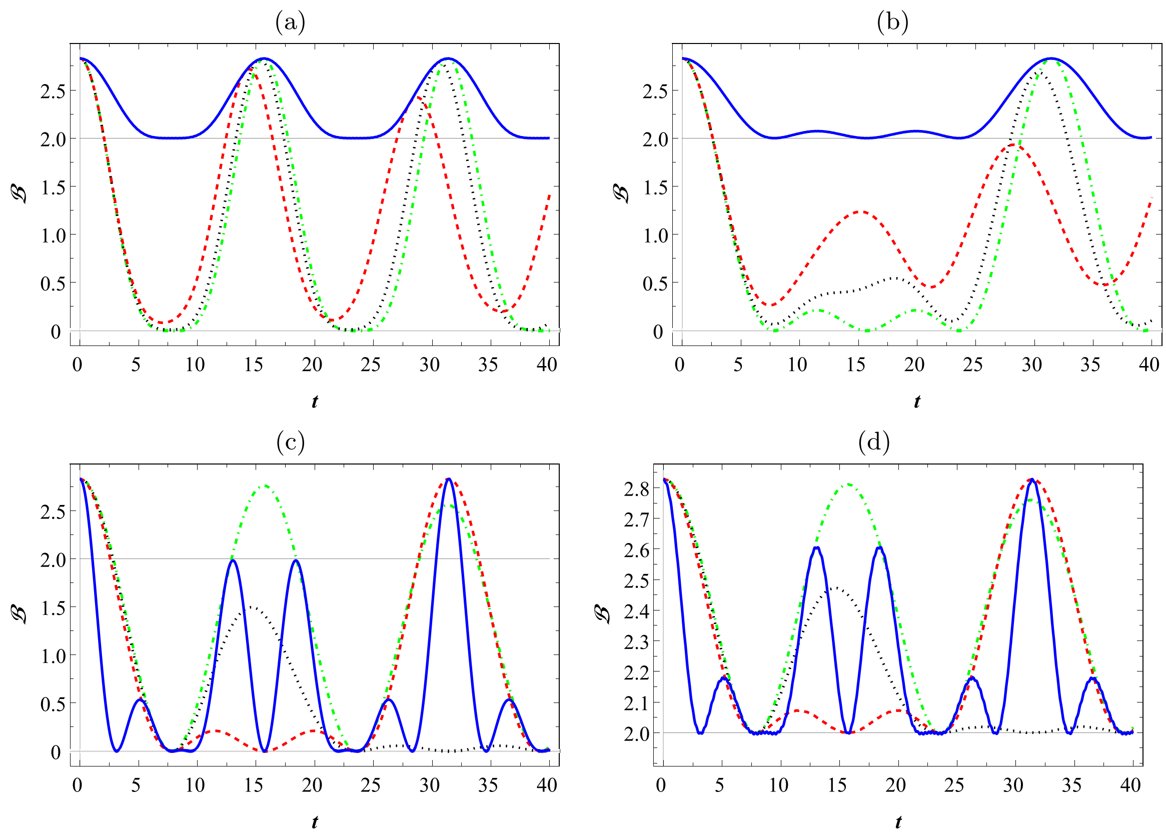

FIG. 7. Bell nonlocality with same parameters as in Fig. 6, where the horizontal line represents the classical limits.

steering and the Bell nonlocality has its maximum violation, where we have a maximally entangled state. Afterwards, the quantum steering decreases as the interaction time increases. The long-lived behavior of Bell nonlocality increases as one increases the external magnetic field. However, in the situation where $\mathbf{B}$ takes the values 0, 0.05, 0.1, the Bell nonlocality disappears before the quantum steering, specifically for symmetry interaction (asymmetry interaction) Bell nonlocality and quantum steering destroyed at $t = 2.1$ ($t = 2.6$) and $t = 2.56$ ($t = 3.23$), respectively, showing that for some ranges of the external magnetic field, the singlet state is steerable and cannot violate the CHSH inequality. On the other hand, when $\mathbf{B} = 10$ for symmetry interaction (asymmetry interaction), the Bell nonlocality and quantum steering disappeared at $t = 6.6$ ($t = 7.5$), meaning that the singlet state is steerable and satisfies Bell nonlocality. Therefore, by increasing $\mathbf{B}$ all steerable states violate the Bell-CHSH inequality.

V. APPLICATION: TELEPORTATION

An entangled mixed state is a valuable resource for exploring the protocol of quantum teleportation [36]. In this study, we aim to investigate how an external magnetic field influences the potential for quantum teleportation within the chosen model. The investigation assumes that the initial input state is

$$|\psi_{\rm in}\rangle = \cos(\theta/2)\,|\downarrow\uparrow\rangle + e^{i\varphi}\sin(\theta/2)\,|\uparrow\downarrow\rangle\,,\quad \forall 0 \leqslant \theta \leqslant \pi,\quad \forall 0 \leqslant \varphi \leqslant 2\pi. \tag{11}$$

Quantum teleportation involves the transformation of an initial input state, denoted $\rho_{\rm in} = |\psi_{\rm in}\rangle\langle\psi_{\rm in}|$, into an output state, denoted $\rho_{\rm out}$, through the action of a mixed channel described by the symbol $\rho_{\rm chl}$. From the mathematical perspective of quantum theory, we can claim that this mixed channel $\rho_{\rm chl}$ is a completely positive map. By using joint measurements and local unitary operations on the input state $\rho_{\rm in}$, we can successfully derive the output state $\rho_{\rm out}$ of the following form:

$$\rho_{\rm out} = \sum_{i,j=0}^{3} p_{ij}(\sigma_i\otimes\sigma_j)\rho_{\rm in}(\sigma_i\otimes\sigma_j), \tag{12}$$

where $\sigma_{1,2,3}$ are the Pauli matrices, σ_0 is the identity matrix and $p_{ij} = p_i p_j = {\rm Tr}[E^i\rho_{\rm chl}]{\rm Tr}[E^j\rho_{\rm chl}]$, the projective measurements E^i are given by means of the four maximally entangled Bell's states as:

$$E^0 = |\Psi^-\rangle\langle\Psi^-|\,,\quad E^1 = |\Phi^-\rangle\langle\Phi^-|\,,\quad E^2 = |\Psi^+\rangle\langle\Psi^+|\,,\quad E^3 = |\Phi^+\rangle\langle\Phi^+|\,. \tag{13}$$

We assume that the quantum channel $\rho_{\rm chl}$ corresponds to the reduced density matrix ρ as described in Eq. (2). However, the fidelity between the initial input state, $\rho_{\rm in}$, and the output state, $\rho_{\rm out}$, can be considered a measure of the quality of the quantum teleportation process. The fidelity is defined as next [37,38]

$$\mathcal{F} = ({\rm Tr}[\sqrt{\sqrt{\rho_{\rm in}}\rho_{\rm out}\sqrt{\rho_{\rm in}}}\,])^2. \tag{14}$$

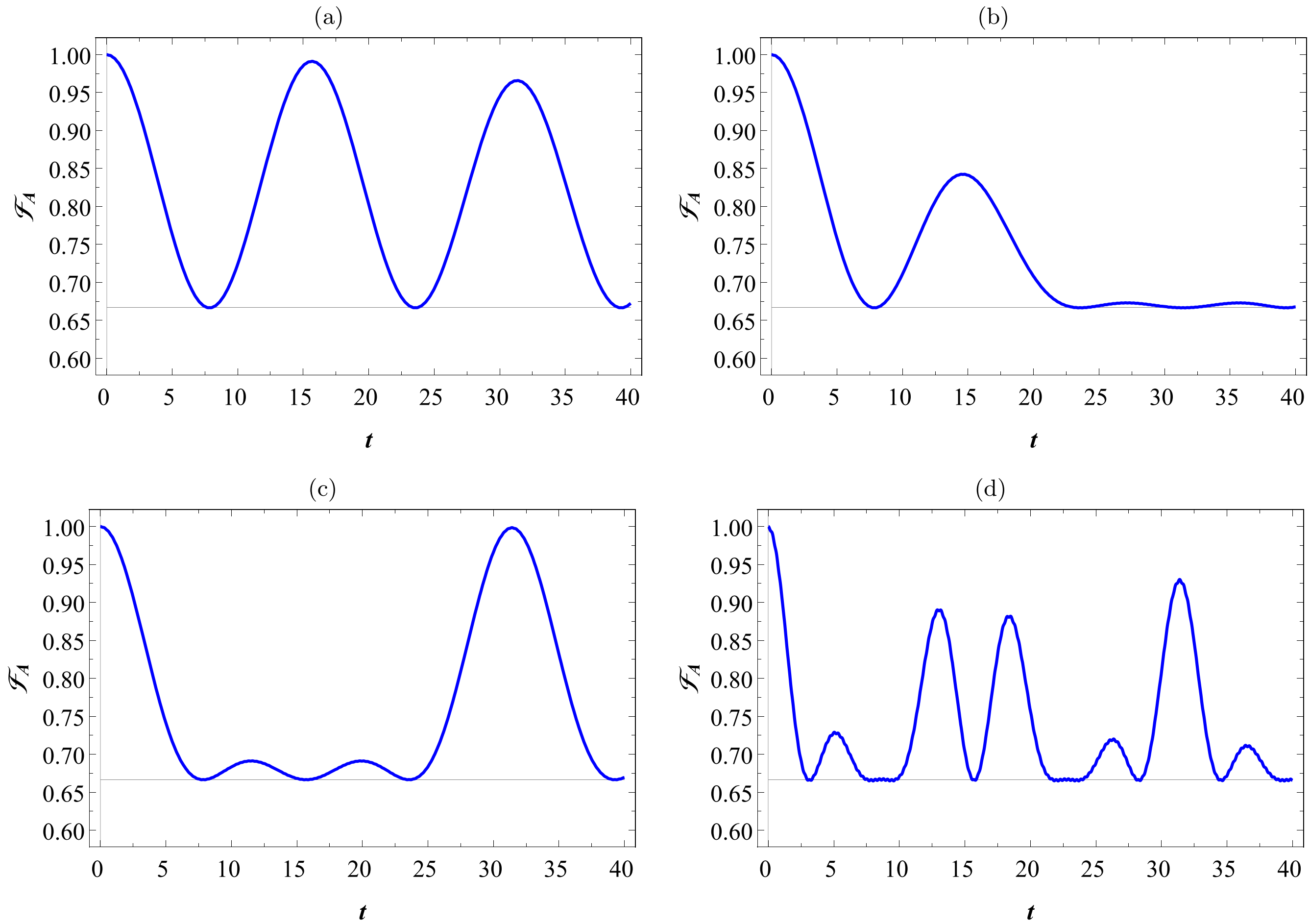

FIG. 8. The average fidelity for fixed external magnetic field $\mathbf{B} = 10$ and $\lambda_{2,1} = 0.2$, where (a) for $\lambda_{1,1} = 0.01$, (b) for $\lambda_{1,1} = 0.05$, (c) for $\lambda_{1,1} = 0.1$, and (d) for $\lambda_{1,1} = 0.5$. The horizontal line represents the classical limit, namely $\mathcal{F} = 2/3$.

Therefore, the average fidelity derived from the fidelity is defined as:

$$\mathcal{F}_A = \frac{1}{4\pi}\int_0^{2\pi} d\varphi \int_0^{\pi} \mathcal{F}\sin(\theta)d\theta. \tag{15}$$

To illustrate how the primary model parameters affect the dynamic behavior of quantum teleportation in a system of two electron spins, each coupled to a proton, we have illustrated the average teleportation fidelity using Eq. (15) in Fig. 8. However, if the average fidelity ($\mathcal{F}_A$) exceeds 2/3, it indicates that the transmission of the quantum state through the quantum protocol is more advantageous compared to classical protocols. The figure shows the variation of the teleportation fidelity for different values of the hyperfine coupling between the first electron and its corresponding proton over the interaction time t. We set $\lambda_{1,2} = 0.2$ and the external magnetic field values to $\mathbf{B} = 10$ in order to specifically explore the relationship between the violation of Bell nonlocality and quantum teleportation. However, initially it is obvious that average fidelity is at its maximum, namely one, as the interaction is switched on $\mathcal{F}_A$ progressively decreased. However, for the situation where $\lambda_{1,1} = 0.01$ ($\lambda_{1,1} \longrightarrow 0$), the $\mathcal{F}_A$ decreases and eventually becomes identical with the classical limits at $t = 7.8$.

As time progresses, there is a periodic, sudden increase in average fidelity accompanied by oscillations, the magnitude of which gradually diminishes. This phenomenon is attributed to the condition $\lambda_{2,1} \gg \lambda_{1,1}$, indicating a strong hyperfine coupling between the second electron and its proton. In other words, the system rapidly loses coherence to the proton, which represents the environment of electron 2 and has a limited capacity to store it. As a result, the system quickly recovers its coherence. The degradation in the magnitude of oscillation is a consequence of the weak coupling between electron 1 and its corresponding proton, meaning the effect of decoherence is slower in this case. Furthermore, in Figs. 8(b) and 8(c), it is obvious that by increasing the values of $\lambda_{1,1}$ the magnitude of oscillations decreases as compared to the last case. Moreover, as $\lambda_{1,1}$ takes a large value, namely 0.5 it is remarkable that oscillation's magnitude cannot reach the maximum value of the $\mathcal{F}_A$ as reached initially. This is because of the strong hyperfine couplings imposed by both protons on their corresponding electrons. In other words, there is always a discrepancy in the feedback of information from the environment; therefore, the dynamics of the system may take a long time to return to its initial state. However, in this section, we have considered the values of the external magnetic field that violate the Bell inequality, which is $\mathbf{B} = 10$, therefore, it is remarkable that the general behavior of the average fidelity is oscillating between its maximum, namely, one, and the classical limits, which are 2/3. By comparing Figs. 7 and 8, one can say that Bell nonlocality, if it is greater than 2, represents a criterion of quantum teleportation.

VI. CONCLUSION

In this paper, we have examined the coherence and quantum correlations within a system composed of two electron spins in a radical pair, where it is assumed that each electron interacts with a corresponding proton. The effect of symmetric and asymmetric configuration and the external magnetic field on the behavior of the quantum correlation quantifiers has been investigated. Moreover, the efficiency of using the generated entangled state between the two spins as a quantum channel to perform quantum teleportation is discussed. The fidelity of the teleported state is quantified at different values of the interaction parameters.

However, our results show that quantum coherence in the absence of the external magnetic field does not ensure the existence of entanglement in the compass system until it exceeds a threshold, namely $\mathcal{C}_l \approx 0.33$. On the other hand, as the value of the external magnetic field increases, it leads to an enhancement of entanglement. In particular, as **B** takes a large value, namely 10, we find that entanglement precisely follows the behavior of quantum coherence; that is, the existence of the latter in the compass system ensures the existence of entanglement. In the absence of an external magnetic field, our results revealed that the singlet state, characterized by Bell nonlocality, can indeed violate the quantum steering inequality. Notably, the opposite scenario does not hold. Furthermore, when the parameter **B** is set to 10, we observe that every singlet state not only exhibits quantum steering but also obeys the principles of Bell nonlocality.

On the other hand, we also examined the effect of symmetric and asymmetric interactions between electrons and their corresponding private environments on the quantumness measures. However, in the case of symmetric interaction, we have found that coherence and nonlocality exhibit a periodic dynamic of sudden death or birth that does depend on the values of the external magnetic field. In contrast, we have shown that the asymmetric interaction between electrons and their environments has a significant effect on the degradation of quantum correlations. We found that the degradation of quantum correlations can be reduced as one increases the strength of the magnetic field.

It is shown that Bell and steerable inequalities behave similarly where the decay, increasing, and the stationary behaviors are predicted on the same interactions. Moreover, the possibility of using the spin state to teleport two-qubit system is examined, where we show that by tuning the coupling parameters, the Bell inequality exceeds its classical bounds, and consequently one can use the spin state for teleportation purposes. However, by controlling the interaction parameters, the fidelity of the teleported state could be above the classical bounds, as well as a long-lived fidelity has been observed at different interaction time.

ACKNOWLEDGMENTS

A.E.A. would like to thank the Max Planck Institute for the Physics of Complex Systems for financial support and the friendly environment. The authors thank the reviewers for their insightful comments.

The authors declare that they have no conflict of interest.

[1] K. Schulten, H. Staerk, A. Weller, H. J. Werner, and B. Nickel, Magnetic field dependence of the geminate recombination of radical ion pairs in polar solvents, Z. Phys. Chem. **101**, 371 (1976).

[2] R. Haberkorn and M. Michel-Beyerle, On the mechanism of magnetic field effects in bacterial photosynthesis, Biophys. J. **26**, 489 (1979).

[3] J. Luo, On the anisotropic weak magnetic field effect in radical-pair reactions, J. Chem. Phys. **158**, 234302 (2023).

[4] U. E. Steiner and T. Ulrich, Magnetic field effects in chemical kinetics and related phenomena, Chem. Rev. **89**, 51 (1989).

[5] K. M. Salikhov, Y. N. Molin, R. Z. Sagdeev, and A. L. Buchachenko, Spin polarization and magnetic effects in radical reactions (Elsevier, Amsterdam, 1984).

[6] Y. Aiache, C. Seida, K. El Anouz, and A. El Allati, Treatment of non-Markovian effects to investigate non-locality, dense coding and non-local information, Phys. Lett. A **496**, 129320 (2024).

[7] S. Haddadi, M. Hadipour, S. Haseli, A. U. Rahman, and A. Czerwinski, Quantum advantages of teleportation and dense coding protocols in an open system, Mathematics **11**, 1407 (2023).

[8] R. Horodecki, P. Horodecki, M. Horodecki, and K. Horodecki, Quantum entanglement, Rev. Mod. Phys. **81**, 865 (2009).

[9] C. Seida, A. El Allati, N. Metwally, and Y. Hassouni, Efficiency increasing of the bidirectional teleportation protocol via weak and reversal measurements, Phys. Scr. **97**, 025102 (2022).

[10] N. Metwally, Estimation of teleported and gained parameters in a non-inertial frame, Laser Phys. Lett. **14**, 049601 (2017).

[11] K. El Anouz, A. El Allati, N. Metwally, and A. S. Obada, The efficiency of fractional channels in the Heisenberg XYZ model, Chaos Solitons Fractals **172**, 113581 (2023).

[12] A. El Allati and M. El Baz, Quantum key distribution using optical coherent states via amplitude damping, Opt. Quantum Electron. **47**, 1035 (2015).

[13] A. El Allati, M. B. Ould Medeni, and Y. Hassouni, Quantum steganography via Greenberger-Horne-Zeilinger GHZ_4 state, Commun. Theor. Phys. **57**, 577 (2012).

[14] J. S. Bell, On the Einstein Podolsky Rosen paradox, Phys. Phys. Fiz. **1**, 195 (1964).

[15] A. Einstein, B. Podolsky, and N. Rosen, Can quantum-mechanical description of physical reality be considered complete? Phys. Rev. **47**, 777 (1935).

[16] E. Schrödinger, Discussion of probability relations between separated systems (Cambridge University Press, Cambridge, 1935).

[17] H. M. Wiseman, S. J. Jones, and A. C. Doherty, Steering, entanglement, nonlocality, and the Einstein-Podolsky-Rosen paradox, Phys. Rev. Lett. **98**, 140402 (2007).

[18] D. J. Saunders, S. J. Jones, H. M. Wiseman, and G. J. Pryde, Experimental EPR-steering using Bell-local states, Nature Phys. **6**, 845 (2010).

[19] S. Wollmann, N. Walk, A. J. Bennet, H. M. Wiseman, and G. J. Pryde, Observation of genuine one-way Einstein-Podolsky-Rosen steering, Phys. Rev. Lett. **116**, 160403 (2016).

[20] J. K. Kalaga, W. Leonński, Jr, and J. Peřina, Einstein-podolsky-rosen steering and coherence in the family of entangled three-qubit states, Phys. Rev. A **97**, 042110 (2018).

[21] Y. Khouja, K. El Anouz, and A. El Allati, A comparative study between EPR steering and directional entanglement of a joint field-field system, Physica A **619**, 128735 (2023).

[22] Y. Khouja and A. El Allati, Quantum steering of two tavis-cummings atoms with dipole-dipole interaction under intrinsic decoherence, Phys. Scr. **98**, 095112 (2023).

[23] R. Uola, A. C. S. Costa, H. C. Nguyen, and O. Gühne, Quantum steering, Rev. Mod. Phys. **92**, 015001 (2020).

[24] H.-J. Werner, Z. Schulten, and K. Schulten, Theory of the magnetic field modulated geminate recombination of radical ion pairs in polar solvents: Application to the pyrene-*N*, *N*-dimethylaniline system, J. Chem. Phys. **67**, 646 (1977).

[25] C. T. Rodgers, S. A. Norman, K. B. Henbest, C. R. Timmel, and P. J. Hore, Determination of radical re-encounter probability distributions from magnetic field effects on reaction yields, J. Am. Chem. Soc. **129**, 6746 (2007).

[26] M. Tiersch, G. G. Guerreschi, J. Clausen, and H. J. Briege, Approaches to measuring entanglement in chemical magnetometers, J. Phys. Chem. A **118**, 13 (2014).

[27] T. Baumgratz, M. Cramer, and M. B. Plenio, Quantifying coherence, Phys. Rev. Lett. **113**, 140401 (2014).

[28] W. K. Wootters, Entanglement of formation of an arbitrary state of two qubits, Phys. Rev. Lett. **80**, 2245 (1998).

[29] K. Bartkiewicz, B. Horst, K. Lemr, and A. Miranowicz, Entanglement estimation from Bell inequality violation, Phys. Rev. A **88**, 052105 (2013).

[30] J. F. Clauser, M. A. Horne, A. Shimony, and R. A. Holt, Proposed experiment to test local hidden-variable theories, Phys. Rev. Lett. **23**, 880 (1969).

[31] R. Horodecki, P. Horodecki, and M. Horodecki, Violating Bell inequality by mixed spin-12 states: Necessary and sufficient condition, Phys. Lett. A **200**, 340 (1995).

[32] E. G. Cavalcanti, S. J. Jones, H. M. Wiseman, and M. D. Reid, Experimental criteria for steering and the Einstein-Podolsky-Rosen paradox, Phys. Rev. A **80**, 032112 (2009).

[33] A. C. S. Costa and R. M. Angelo, Quantification of Einstein-Podolsky-Rosen steering for two-qubit states, Phys. Rev. A **93**, 020103(R) (2016).

[34] X. G. Fan, H. Yang, F. Ming, Z. Y. Ding, D. Wang, and L. Ye, Universal complementarity between coherence and intrinsic concurrence for two-qubit states, New J. Phys. **21**, 093053 (2019).

[35] Z. B. Walters, Quantum dynamics of the avian compass, Phys. Rev. E **90**, 042710 (2014).

[36] Y. Yeo, Teleportation via thermally entangled states of a two-qubit Heisenberg *XX* chain, Phys. Rev. A **66**, 062312 (2002).

[37] Y. C. Liang, Y. H. Yeh, P. E. M. F. Mendonça, R. Y. Teh, M. D. Reid, and P. D. Drummond, Quantum fidelity measures for mixed states, Rep. Prog. Phys. **82**, 076001 (2019).

[38] K. El Anouz, A. El Allati, and F. Saif, Study different quantum teleportation amounts by solving Lindblad master equation, Phys. Scr. **97**, 035102 (2022).